




Article

Impacts of Bacteriostatic and Bactericidal Antibiotics on the Mitochondria of the Age-Related Macular Degeneration Cybrid Cell Lines

Nasim Salimiaghdam ¹, Lata Singh ¹ , Mithalesh K. Singh ¹ , Marilyn Chwa ¹, Shari R. Atilano ¹, Zahra Mohtashami ¹ , Anthony B. Nesburn ^{1,2}, Baruch D. Kuppermann ¹, Stephanie Y. Lu ¹ and M. Cristina Kenney ^{1,3,*}

¹ Department of Ophthalmology, Gavin Herbert Eye Institute, University of California Irvine, Irvine, CA 92697, USA; salimiag@hs.uci.edu (N.S.); drlata.singh@aaims.edu (L.S.); mithales@hs.uci.edu (M.K.S.); mchwa@hs.uci.edu (M.C.); satilano@hs.uci.edu (S.R.A.); zmohtash@hs.uci.edu (Z.M.); anesburn@hs.uci.edu (A.B.N.); bdkupper@hs.uci.edu (B.D.K.); sylu@hs.uci.edu (S.Y.L.)

² Cedars-Sinai Medical Center, Los Angeles, CA 90048, USA

³ Department of Pathology and Laboratory Medicine, University of California Irvine, Irvine, CA 92697, USA

* Correspondence: mkenney@hs.uci.edu; Tel.: +949-824-7603; Fax: +949-824-9626

Abstract: We assessed the potential negative effects of bacteriostatic and bactericidal antibiotics on the AMD cybrid cell lines (K, U and J haplogroups). AMD cybrid cells were created and cultured in 96-well plates and treated with tetracycline (TETRA) and ciprofloxacin (CPFX) for 24 h. Reactive oxygen species (ROS) levels, mitochondrial membrane potential ($\Delta\psi$ M), cellular metabolism and ratio of apoptotic cells were measured using H2DCFDA, JC1, MTT and flow cytometry assays, respectively. Expression of genes of antioxidant enzymes, and pro-inflammatory and pro-apoptotic pathways were evaluated by quantitative real-time PCR (qRT-PCR). Higher ROS levels were found in U haplogroup cybrids when treated with CPFX 60 μ g/mL concentrations, lower $\Delta\psi$ M of all haplogroups by CPFX 120 μ g/mL, diminished cellular metabolism in all cybrids with CPFX 120 μ g/mL, and higher ratio of dead cells in K and J cybrids. CPFX 120 μ g/mL induced overexpression of *IL-33*, *CASP-3* and *CASP-9* in all cybrids, upregulation of *TGF- β 1* and *SOD2* in U and J cybrids, respectively, along with decreased expression of *IL-6* in J cybrids. TETRA 120 μ g/mL induced decreased ROS levels in U and J cybrids, increased cellular metabolism of treated U cybrids, higher ratio of dead cells in K and J cybrids and declined $\Delta\psi$ M via all TETRA concentrations in all haplogroups. TETRA 120 μ g/mL caused upregulation of *IL-6* and *CASP-3* genes in all cybrids, higher *CASP-7* gene expression in K and U cybrids and downregulation of the *SOD3* gene in K and U cybrids. Clinically relevant dosages of ciprofloxacin and tetracycline have potential adverse impacts on AMD cybrids possessing K, J and U mtDNA haplogroups in vitro.

Keywords: AMD cybrids; mtDNA haplogroups; antibiotics; bacteriostatic; bactericidal



Citation: Salimiaghdam, N.; Singh, L.; Singh, M.K.; Chwa, M.; Atilano, S.R.; Mohtashami, Z.; Nesburn, A.B.; Kuppermann, B.D.; Lu, S.Y.; Kenney, M.C. Impacts of Bacteriostatic and Bactericidal Antibiotics on the Mitochondria of the Age-Related Macular Degeneration Cybrid Cell Lines. *Biomolecules* **2022**, *12*, 675. <https://doi.org/10.3390/biom12050675>

Academic Editors: Stephanie C. Joachim and Sven Schnichels

Received: 27 March 2022

Accepted: 3 May 2022

Published: 7 May 2022

Publisher's Note: MDPI stays neutral with regard to jurisdictional claims in published maps and institutional affiliations.



Copyright: © 2022 by the authors. Licensee MDPI, Basel, Switzerland. This article is an open access article distributed under the terms and conditions of the Creative Commons Attribution (CC BY) license (<https://creativecommons.org/licenses/by/4.0/>).

1. Introduction

The introduction of antibiotics in the 20th century is considered an astounding breakthrough in medicine [1]. Antibiotics cure a wide range of infectious diseases, and they facilitate the success of modern medical procedures such as organ transplantations, surgeries and cancer therapy regarding prevention of opportunistic infections [2]. However, over time, the growing pattern of antimicrobial resistance (AMR) and some remarkable adverse effects resulting from administration or misuse of antibiotics have attracted attention [3]. Fluoroquinolones are antibiotics frequently used in medical and surgical fields, such as ophthalmology. These bactericidal agents (e.g., norfloxacin, lomefloxacin, ciprofloxacin and ofloxacin) have broad-spectrum antibacterial activity, and can be administered via topical, intravitreal and systemic routes [4]. Their principal mechanism of action

is inhibiting DNA topoisomerases and preventing bacterial DNA replication by impeding mitochondrial DNA replication, transcription and lowering mtDNA copy number [5]. Although fluoroquinolones are well-tolerated agents overall, they have induced some serious side effects in some individuals, such as tendinopathy, cardiac arrhythmia and optic neuropathy [6–8]. Fife and colleagues conducted a case–control study on ophthalmologic patients exposed to fluoroquinolones, who were observed for an average of 27 months. An association between exposure with fluoroquinolones and risk of retinal detachment was demonstrated [9].

Tetracyclines (e.g., tetracycline, demeclocycline, minocycline and doxycycline) are well-established bacteriostatic agents affecting a wide array of Gram-positive and Gram-negative bacteria [10]. Tetracyclines have been effective in the prevention and treatment of allergic, inflammatory, immune and infectious diseases, such as chronic blepharitis, scleroderma and pyoderma gangrenosum [11–13]. Tetracycline derivatives have a high affinity to bacterial ribosome 30S subunit. Therefore, their mechanism of action is blocking the bacterial protein synthesis process by preventing the association between aminoacyl-tRNA and bacterial ribosome 30S subunits [14]. Considering the negative impacts of tetracyclines on matrix metalloproteinases (MMPs), mast cells and production of inflammatory cytokines, studies have demonstrated the possible therapeutic role of these agents against COVID-19 [15–17]. In terms of adverse effects of tetracyclines, studies have revealed their potential side effects such as phototoxic dermatitis, gastrointestinal disturbance and discoloration of teeth and oral cavity [18,19]. Wallace et al. reported the reduction in intraocular pressure of cats resulting from intraocular injection of tetracycline derivatives, particularly demeclocycline [20].

Mitochondria are intracellular organelles which are the main source of energy metabolism in eukaryote cells via ATP production [21]. Moreover, mitochondria are involved in numerous essential intracellular reactions such as ROS production, apoptosis, synthesis of lipids and steroids, breaking down of sugars and fatty acid oxidation [22]. The hypothesis of an endosymbiotic origin of mitochondria occurring billion years ago has been discussed in previous studies [23]. Later studies indicated remarkable similarities between bacteria and mitochondria with respect to their sizes, circular DNA, ribosomal subunits and electron transport chain [24,25]. Previous in vitro studies showed the detrimental anti-mitochondrial outcomes of antibiotics. Kalghatgi and colleagues conducted a study using bactericidal and bacteriostatic antibiotics on the peripheral blood cells of mice. Authors treated the mice with kanamycin (25 µg/mL), ampicillin (20 µg/mL) and ciprofloxacin (10 µg/mL) along with tetracycline (10 µg/mL). They found that cells treated with bactericidal agents showed disrupted mitochondrial electron transport chain leading to higher ROS production [26]. Patients suffering from age-related macular degeneration (AMD) showed a higher level of retinal mitochondrial DNA (mtDNA) abnormalities such as deletions [27]. Therefore, the harmful effects of antibiotics on damaged mitochondria might be more crucial in these individuals.

In our previous study conducted on ARPE-19 (human retinal pigment epithelial) cell lines, we found significantly decreased levels of $\Delta\psi_M$ and cellular metabolism after TETRA and CPFY treatments. Furthermore, overexpression of apoptotic (*CASP-7*, *CASP-9* and *BAX*) and inflammatory (*IL-6*) pathway genes was induced by exposure to CPFY [28]. Moreover, our recent study performed on MIO-M1 (human retinal Müller) cells treated with CPFY and TETRA showed CPFY induced lower levels of cellular metabolism, $\Delta\psi_M$ and ROS along with overexpression of *CASP-3* and *CASP-9* [29].

Age-related macular degeneration (AMD) is a retinal degenerative disease, affected by various genetic and environmental risk factors which cause progressive vision loss in the elderly population of developed countries [30,31]. AMD cybrids are cell lines that have identical nuclei but mitochondria from different individuals. Analyses of the mtDNA showed that AMD is associated with the J, T and U haplogroups but individuals with the H haplogroup are at low risk for developing AMD [32]. Mitochondrial DNA variants of respiratory complex I that uniquely characterize haplogroup T2 are associated with

increased risk of age-related macular degeneration [33]. Kenney et al. demonstrated that mtDNA haplogroups have key roles in numerous molecular pathways associated with AMD progression such as energy production, cell growth and signaling [34].

In this study, our aim is to assess the potential damaging effects of CPF and TETRA on the cellular health and mitochondria of AMD cybrid cell lines.

2. Materials and Methods

2.1. Ethic Statement

This study involving human subjects was performed according to stated principals in Declaration of Helsinki. After obtaining the informed written consent, the Institutional Review Board of the University of California, Irvine approved the research (UCI IRB #2003-3131).

2.2. Cybrids Creation

The process of creation of trans-mitochondrial cybrids is described in previous studies [33]. After collecting 10 mL of peripheral blood using tubes with sodium citrate, DNA extraction kits (Puregene, Qiagen, Valencia, CA, USA) and the Nanodrop 1000 (Thermo Scientific, Wilmington, DE, USA) were used for DNA isolation and quantification, respectively. Then, a series of centrifuge steps were performed for platelet isolation followed by using Tris buffer saline (TBS) for platelet suspension. ARPE-19 cell lines, purchased from ATCC (Manassa, VA, USA), demonstrated similar functional and structural characteristics to in vivo RPE cells [35]. The ARPE-19 were exposed to low-dose ethidium bromide and serially passaged until they were deficient in mtDNA (Rho0) [36]. As described in previous studies, cybrids were created by fusion of Rho0 ARPE-19 cells with platelets using polyethylene glycol [32].

2.3. Cybrids Culture Conditions

For culturing the cybrids, DMEM-F12 serum media contained 10% dialyzed fetal bovine serum, 17.5 mM glucose, 2.5 µg/mL fungizone, 100 µg/mL streptomycin, 50 µg/mL gentamycin, 100 unit/mL penicillin and 50 µg/mL gentamycin. Experiments examined a total of 8 cybrid cell lines that originated from different individuals with AMD (K cybrids, $n = 3$; U cybrids, $n = 3$ and J cybrids, $n = 2$). For all experiments, only passage 5 cybrid cell lines were used. After being plated, the cultures were not treated until the cybrid cells reached confluency. Table 1 illustrates the epidemiological information of the cybrids used in this study.

Table 1. Demographics of the K, U and J cybrids.

Cybrid	Haplogroup	Age	Sex	Ethnicity	Diagnosis
16-188	K	90	M	Caucasian	Dry AMD
13-129	K1a1b1a	89	M	Caucasian	Wet AMD
16-187	K2a2a1	82	M	Caucasian	Dry AMD
14-138	U2e1a1	69	M	Caucasian	Dry AMD
17-200	U	69	M	Caucasian	Dry AMD
18-238	U	76	F	Caucasian	Wet AMD
14-136	J2a1a1a2	77	F	Caucasian	Wet AMD
14-142	J1c2g	91	F	Caucasian	Wet AMD

2.4. Intracellular Level of Reactive Oxygen Species (ROS Assay)

For performing ROS, JC-1 and MTT assays, the cybrid cell lines were placed in 96-well plates (10^4 cells/well) and incubated in 37 °C for 24 h. Then, cells were treated with antibiotics and cultured for an additional 48 h. ROS was measured by adding 100 µL/well

H2DCFDA solution (2',7'-dichlorhydrofluorescein diacetates; Catalog# D399, Thermo Fisher Scientific, Waltham, MA, USA). The presence of intracellular ROS induces conversion of the dye to fluorescent molecules. The fluorescent plate reader (SoftMax Pro, version 6.4, Catalog# 94089, Sunnyvale, CA, USA) was used to measure the excitation (492 nm) and emission (520 nm) wavelengths. For the ROS assay, there were four TETRA groups: vehicle-control (Meth), TETRA (30 µg/mL, 60 µg/mL and 120 µg/mL); and four CPFX groups: Vehicle-control (HCl), CPFX (30 µg/mL, 60 µg/mL and 120 µg/mL). Entire experiments were repeated 3 times.

2.5. Mitochondria Membrane Potential ($\Delta\psi$ M) (JC-1 Assay)

Cells were cultured in 96-well plates (10^4 cells/well). After adding the JC-1 reagent (5,5',6,6'-tetrachloro-1,1',3,3'-tetraethyl-benzimidazolylcarbocyanine iodide; Catalog# 30001, Biotium, CA, USA) to each well, plates were read using the fluorescent plate reader (SoftMax Pro, version 6.4, Catalog# 94089, Sunnyvale, CA, USA). The green (EX 485 nm and EM 535 nm) and red (EX 550 nm and EM 600 nm) emissions were used for measuring the ratio of red to green fluorescent. For the JC-1 experiments, there were four TETRA groups: vehicle-control (Meth), TETRA (30 µg/mL, 60 µg/mL and 120 µg/mL); and four CPFX groups: Vehicle-control (HCl), CPFX (30 µg/mL, 60 µg/mL and 120 µg/mL). Entire experiments were repeated 3 times.

2.6. Cellular Metabolism Assay (MTT Assay)

For measuring levels of cellular metabolism, the MTT assay was performed using 96-well plates. An amount of 10 µL MTT assay reagent (3-(4,5-Dimethylthiazol-2-yl)-2,5-diphenyltetrazolium bromide; Catalog# 30006, Biotium, CA, USA) was added to each well containing cultured cybrids (10^4 /well). After 2 h incubation in 37 °C, 100 µL DMSO was added to each well. Then, Biotek Elx808 Absorbance Reader, (Winooski, VT, USA) was used to analyze the plates. For the MTT experiments, there were four TETRA groups (vehicle-control (Meth), TETRA (30 µg/mL, 60 µg/mL and 120 µg/mL)) and four CPFX groups (vehicle-control (HCl), CPFX (30 µg/mL, 60 µg/mL and 120 µg/mL)). Experiments were repeated 3 times.

2.7. The Ratio of Live, Apoptotic and Dead Cells (Flow Cytometry)

To measure the ratio of live and apoptotic cells affected by exogenous 120 µg/mL CPFX and TETRA treatments, cells were cultured in 6-well plates (50,000/well) and incubated for 24 h. After 48 h treatment period with antibiotics, 50 µL propidium iodide (PI, representing dead cells) and YO-PRO-1 (an early marker for apoptosis) stains were added to seeded cells. Cells were incubated for 30 min on ice followed by flow cytometry analyses (Flow Cytometer, Novocyte 3000; Catalog# 4355488, San Diego, CA, USA). The flow cytometry values were measured using 488 nm excitation with green fluorescence emission for YO-PRO[®]-1 dye (i.e., 530/30 bandpass) and red fluorescence emission for propidium iodide (i.e., 610/20 bandpass). This technique measures the physical and chemical characteristics of the cells such as the proportion of live, apoptotic and dead cells in untreated, vehicle-control and antibiotic-treated (CPFX and TETRA) groups. To accomplish standard compensation, single-colored stained cells were used. To assure a statistically significant determination of a sample volume, 10,000 bead events were collected per each sample.

2.8. Isolation of RNA and cDNA Amplification

Cultured cybrids in 6-well plates were treated with 120 µg/mL CPFX and TETRA. After 48 h incubation period, RNA was isolated from the cell lysis using the RNeasy Mini-Extraction kit (Puregene, Qiagen, Valencia, CA, USA). Nano Drop 1000 (Thermo Scientific, Wilmington, DE, USA) was used for RNA quantification. Then, each isolated RNA was reverse transcribed to complementary DNA (cDNA) by using Superscript IV VILO Master Mix with the DNase Enzyme (ThermoFisher, Waltham, MA, USA).

2.9. Quantitative Real Time Polymerase Chain Reaction (qRT-PCR)

Isolation of total RNA was performed from cultured CPFEX-exposed ($n = 3$), TETRA-exposed ($n = 3$), associated vehicle-control (HCl and TETRA) ($n = 3$) and untreated ($n = 3$) cells. Table 2 demonstrates all target primers, which are pre-designed via Qiagen QuantiTect Primer Assays or KiCqStart SYBR[®] Green primers (Sigma–Aldrich, Burlington, MA, USA). PowerUp SYBR Green Master Mix (ThermoFisher) on a ThermoFisher Quant Studio 3 Real-Time PCR System was used for performing qRT-PCR, which evaluated the relative expression level of various genes associated with pro-inflammatory (*IL-6*, *IL-33* and *TGF- β 1*), pro-apoptotic (*CASP-3*, *CASP-7* and *CASP-9*) and antioxidant enzyme (*SOD2*, *SOD3* and *GPX3*) pathways genes. In this study, the housekeeping gene was *HPRT1*, which is an enzyme recycling inosine and guanine in the purine salvage pathway and is considered a stable endogenous control gene when investigating alterations in gene expression. Therefore, as a consistent endogenous control, *HPRT1* primer was used as the reference gene for reaching a standard expression level for all primers [37]. The $\Delta\Delta C_t$ method was used for analyzing the data, in which $\Delta C_t = [C_t \text{ (threshold value) of the target gene}] - [C_t \text{ for } HPRT1]$, and $\Delta\Delta C_t = \Delta C_t \text{ of the treatment condition} - \Delta C_t \text{ of the untreated condition}$. When comparing the treated conditions to untreated conditions, the fold changes were measured as: $\text{fold change} = 2^{-\Delta\Delta C_t}$. Triplicate formats of antibiotic treated cells (CPFEX and TETRA) compared to untreated and vehicle-control (HCl and Meth) samples were analyzed.

2.10. Statistical Analyses

GraphPad Prism (Version 5.0, GraphPad Software, Inc., San Diego, CA, USA) was used for statistical analyses. One-way ANOVA Tukey test was performed when comparing the differences among untreated, vehicle-control (HCl and Meth) and antibiotic-treated (CPFEX and TETRA) cells. The p value of less than 0.05 was considered statistically significant. Three replicates were allocated for each condition in this study and the associated data analyzed in triplicate.

Table 2. Information of the genes associated with inflammatory, apoptotic and antioxidant enzymes pathways in AMD cybrid cells.

Symbol	Gene Name	GenBank Accession No.	Sigma Primer Sequences Or Qiagen Gene Globe ID	Function
<i>CASP-3</i>	Caspase 3, apoptosis-related cysteine peptidase	NM_004346 NM_032991	QT00023947	Encodes protein as a cysteine–aspartic acid protease that plays a central role in the execution phase of cell apoptosis.
<i>CASP-7</i>	Caspase 7, apoptosis-related cysteine peptidase	NM_145248, XM_006725153, XM_006725154, XM_005268295, XM_006725155, XM_005268294, XM_006719962	QT00003549	This gene encodes a member of the cysteine–aspartic acid protease (caspase) family. Sequential activation of caspases plays a central role in the execution phase of cell apoptosis.
<i>CASP-9</i>	Caspase 9, apoptosis-related cysteine peptidase	NM_001229 NM_032996	QT00036267	Encodes a member of the cysteine–aspartic acid protease (caspase) family, which is involved in the execution phase of cell apoptosis.
<i>IL-6</i>	Interleukin 6	NM_000600	FH1-5'-GCAGAAAAAGGCAAAGAATG-3' RH1-5'-CTACATTTGCCGAAGAGC-3'	This gene encodes a cytokine that functions in inflammation and the maturation of B cells. In addition, the encoded protein has been shown to be an endogenous pyrogen capable of inducing fever in people with autoimmune diseases or infections.
<i>IL-33</i>	Interleukin 33	NM_033439 NM_001199640 NM_001127180	FH1-5'-CCAGAAGTCTTTTGTAGG-3' RH1-5'-GCTGGGAAATAAGGTGTT-3'	The protein encoded by this gene is a cytokine that binds to the IL1RL1/ST2 receptor. The encoded protein is involved in the maturation of Th2 cells and the activation of mast cells, basophils, eosinophils and natural killer cells.
<i>TGF-β1</i>	Transforming growth factor beta-1-like	NM_003238	FH1-5'-AACCCACAACGAAATCTATG-3' RH1-5'-CTTTTAACCTTGAGCCTCA-GC-3'	This gene is a polypeptide member of the transforming growth factor beta superfamily of cytokines. It is a secreted protein that performs many cellular functions, including the control of cell growth, cell proliferation, cell differentiation and apoptosis.
<i>SOD1</i>	Superoxide dismutase 1	NM_000454	QT01671551	This gene is a member of the iron/manganese superoxide dismutase family. The protein encoded by this gene is a soluble cytoplasmic protein, acting as a homodimer to convert naturally occurring but harmful superoxide radicals to molecular oxygen and hydrogen peroxide.

Table 2. Cont.

Symbol	Gene Name	GenBank Accession No.	Sigma Primer Sequences Or Qiagen Gene Globe ID	Function
<i>SOD2</i>	Superoxide dismutase 2	NM_000636	FH1-5'-ATCTACCCTAATGATCCCAG-3' RH1-5'-AGGACCTTATAGGGTTTTTCAG-3'	This gene encodes a mitochondrial protein that forms a homotetramer and binds one manganese ion per subunit. This protein binds to the superoxide byproducts of oxidative phosphorylation and converts them to hydrogen peroxide and diatomic oxygen.
<i>SOD3</i>	Superoxide dismutase 3	NM-003102	QT01664327	This gene encodes a member of the superoxide dismutase (SOD) protein family, which catalyzes the conversion of superoxide radicals into hydrogen peroxide and oxygen, effective in protection of the brain, lungs and other tissues from oxidative stress.
<i>GPX3</i>	Glutathione peroxidase 3	NM_002084	FH1-5'-GCAACCAATTTGGAAAACAG-3' RH1-5'-CTCAAAGAGCTGGAAATTAGG-3'	The protein encoded by this gene belongs to the glutathione peroxidase family, members of which catalyze the reduction of organic hydroperoxides and hydrogen peroxide (H ₂ O ₂) by glutathione, and thereby protect cells against oxidative damage. Several isozymes of this gene family exist in vertebrates, which vary in cellular location and substrate specificity.
<i>HPRT1</i>	Hypoxanthine Phosphoribosyl transferase 1	NM_000194	FH1-5'-ATAAGCCAGACTTTGTTGG-3' RH1-5'-ATAGGACTCCAGATGTTTCC-3'	The protein encoded by this gene is a transferase, which catalyzes conversion of hypoxanthine to inosine monophosphate and guanine to guanosine monophosphate via transfer of the 5-phosphoribosyl group from 5-phosphoribosyl 1-pyrophosphate. This enzyme plays a central role in the generation of purine nucleotides through the purine salvage pathway.

3. Results

3.1. ROS Levels

First, we compared the effect of antibiotics on the oxidative stress in the cells of different cybrid haplogroups. In terms of intracellular ROS levels, the different mtDNA haplogroups cybrids demonstrated varying results. After treatment with 60 $\mu\text{g}/\text{mL}$ CPF, U cybrids showed increased ROS levels ($p < 0.05$) (Figure 1b). In contrast, CPF-treated J cybrids showed decreased ROS levels caused by CPF 120 $\mu\text{g}/\text{mL}$ ($p < 0.05$), (Figure 1c). Similarly, TETRA 120 $\mu\text{g}/\text{mL}$ decreased ROS levels ($p < 0.001$) in J cybrids (Figure 1c). Furthermore, neither of the antibiotics affected the ROS levels in treated K haplogroups (Figure 1a). These results indicate that higher dosages of these antibiotics could have impacts on the ROS levels in U and J haplogroups.

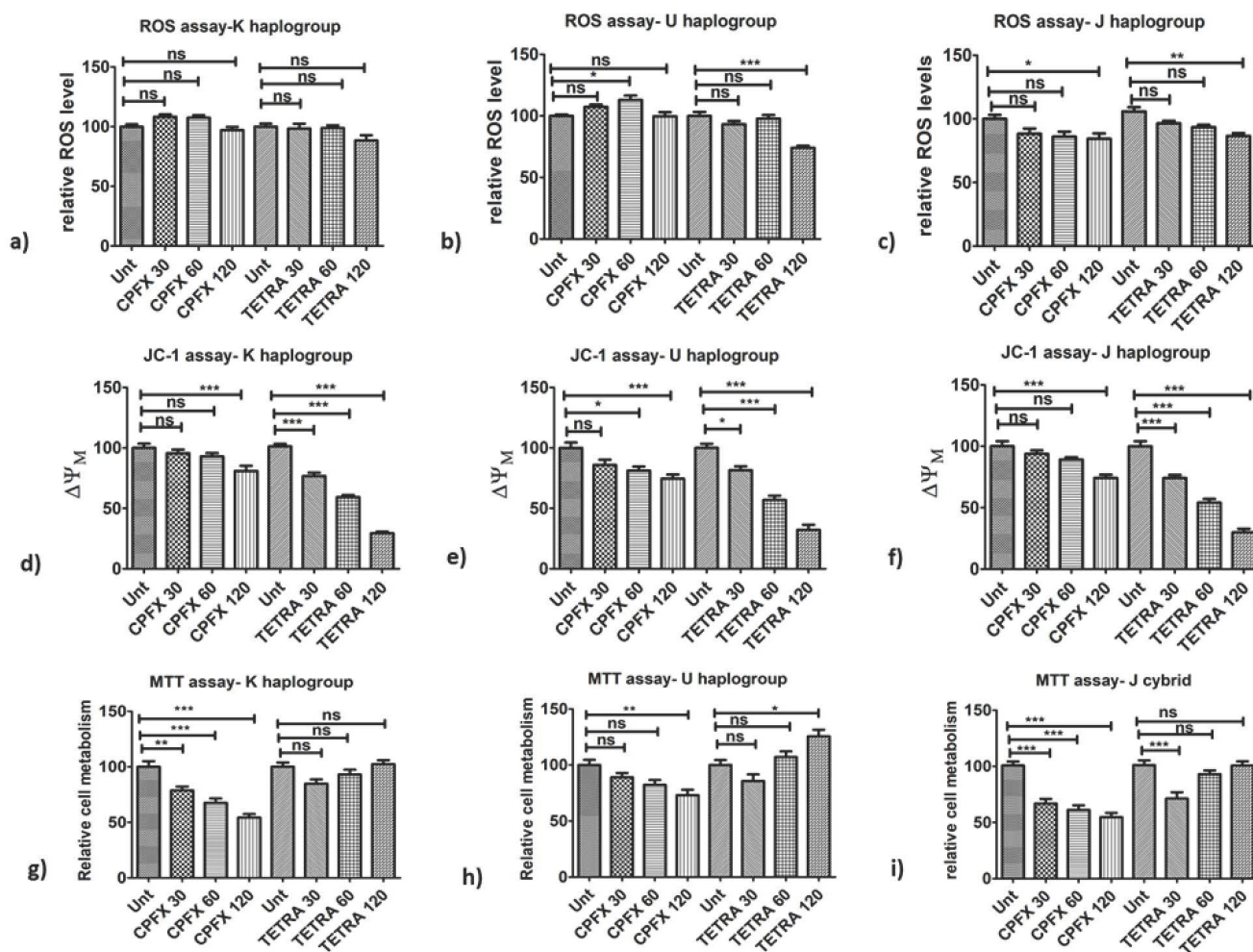


Figure 1. Impacts of CPF and TETRA on ROS levels, $\Delta\psi\text{M}$ and cellular metabolism of K, U and J cybrids via ROS, JC-1 and MTT assays. (a) no changes in ROS levels via neither antibiotics in K cybrids; (b) CPF 60 $\mu\text{g}/\text{mL}$ increased ROS levels in U cybrids and diminished via TETRA 120 $\mu\text{g}/\text{mL}$; (c) ROS levels reduced by CPF and TETRA 120 $\mu\text{g}/\text{mL}$ in J cybrids; (d) CPF 120 $\mu\text{g}/\text{mL}$ and all TETRA treatments reduced $\Delta\psi\text{M}$ in K cybrids; (e) $\Delta\psi\text{M}$ diminished via CPF 60 and 120 $\mu\text{g}/\text{mL}$ and all TETRA concentrations in U cybrids; (f) CPF 120 $\mu\text{g}/\text{mL}$ along with all TETRA concentrations decreased $\Delta\psi\text{M}$ in J cybrids; (g) Diminished cellular metabolism with all CPF concentrations in K cybrids; (h) CPF 120 $\mu\text{g}/\text{mL}$ reduced cellular metabolism of U cybrids but higher level with TETRA 120 $\mu\text{g}/\text{mL}$; (i) All CPF treatments and TETRA 30 $\mu\text{g}/\text{mL}$ declined cellular metabolism of J cybrids. (* $p < 0.05$, ** $p < 0.01$, *** $p < 0.0001$).

3.2. Alterations of Mitochondrial Membrane Potential ($\Delta\psi$ M)

Next, we investigated the impact of antibiotics on the $\Delta\psi$ M of different cybrid haplogroups. The $\Delta\psi$ M levels were decreased by both CPFEX and TETRA treatments. The CPFEX 120 $\mu\text{g}/\text{mL}$ decreased $\Delta\psi$ M in K cybrids ($p < 0.0001$) (Figure 1d). The U cybrids treated with 60 ($p < 0.05$) and 120 $\mu\text{g}/\text{mL}$ CPFEX ($p < 0.0001$) showed decreased $\Delta\psi$ M, respectively (Figure 1e). Moreover, $\Delta\psi$ M levels were lower in J cybrids treated with CPFEX 120 $\mu\text{g}/\text{mL}$ ($p < 0.0001$) (Figure 1f). All TETRA treatment concentrations caused significant reduction in $\Delta\psi$ M in all cybrid groups. In K cybrids treated with TETRA 30, 60 and 120 $\mu\text{g}/\text{mL}$ ($p < 0.0001$), there was a remarkable reduction in $\Delta\psi$ M (Figure 1d). Furthermore, $\Delta\psi$ M levels were decreased in U cybrids via TETRA 30 $\mu\text{g}/\text{mL}$ ($p < 0.05$) along with TETRA 60 and 120 $\mu\text{g}/\text{mL}$ ($p < 0.0001$) (Figure 1e). Moreover, J cybrids treated with TETRA 30, 60 and 120 $\mu\text{g}/\text{mL}$ ($p < 0.0001$) showed significantly reduced levels of $\Delta\psi$ M (Figure 1f). These results demonstrated that higher treatment concentrations of CPFEX and all treatment concentrations of TETRA negatively affected the exposed K, U and J cybrids.

3.3. Changes in Cellular Metabolism (MTT Assay)

We then investigated whether antibiotic treatment has an influence on the cellular metabolism of a cybrid with different haplogroups. In cultured K cybrids, CPFEX 30 $\mu\text{g}/\text{mL}$ ($p < 0.01$), 60 $\mu\text{g}/\text{mL}$ ($p < 0.0001$) and 120 $\mu\text{g}/\text{mL}$ ($p < 0.0001$) decreased cellular metabolism (Figure 1g). Exposure to CPFEX 120 $\mu\text{g}/\text{mL}$ ($p < 0.01$) decreased cellular metabolism of U cybrids (Figure 1h). Interestingly, the U cybrids showed higher cell metabolism when treated with TETRA 120 $\mu\text{g}/\text{mL}$ ($p < 0.05$) compared to the vehicle-control-treated cybrid (Figure 1h). When J cybrids were treated with CPFEX 30, 60 or 120 $\mu\text{g}/\text{mL}$, there were significantly diminished levels of cellular metabolism ($p < 0.0001$) (Figure 1i). The TETRA 30 $\mu\text{g}/\text{mL}$ also lowered the metabolism of exposed cybrids ($p < 0.0001$) (Figure 1i). These results demonstrate that CPFEX and TETRA have detrimental effects on the cellular metabolism.

3.4. Ratio of Apoptosis and Dead Cells (Flowcytometry)

We investigated whether apoptotic cell death contributes to the negative impact of antibiotics on the different haplogroup cybrids. In K cybrids, treatment with 120 $\mu\text{g}/\text{mL}$ of CPFEX induced 100% value dead cells ($p < 0.0001$), versus 9.53% dead cells induced by vehicle-control treatment (Figure 2a,d). The TETRA-treated cells showed 18.66% ($p < 0.05$) dead cells versus 15.98% for the vehicle-control treated cells (Figure 2g,j). In U cybrids, there was no significant alteration of the ratio of dead cells with neither CPFEX (17.81%) (Figure 2b,e) and TETRA (25.12%) (Figure 2h,k) versus HCl (15.64%) and Meth (23.61%)-exposed cells, respectively. Compared to vehicle-control-exposed cells, the J cybrids treated with CPFEX 120 $\mu\text{g}/\text{mL}$ showed a substantial increase in relative dead cells (90.52% versus 25.40%) ($p < 0.05$) (Figure 2c,f). The TETRA-treated cells also showed an increase in dead cells (16.36% versus 6.47%) ($p < 0.05$) compared to vehicle-control treated cells (Figure 2i,l). Therefore, CPFEX and TETRA significantly increase the proportion of apoptotic and finally dead cells.

3.5. Alterations of Pro-Inflammatory, Pro-Apoptotic and Antioxidant Enzymes Genes

Next, we evaluated the effects of the antibiotics on the different cybrids at the gene level.

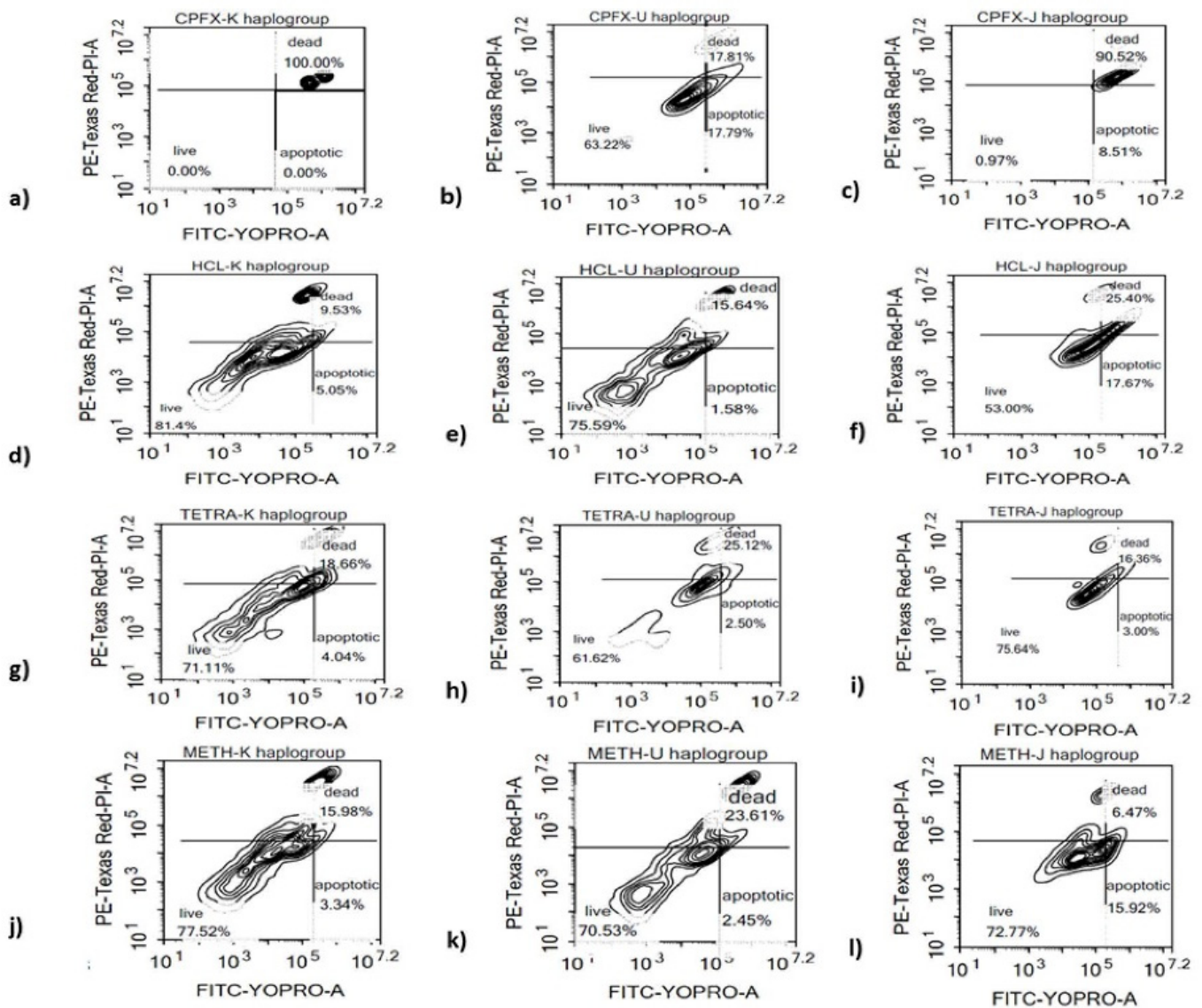


Figure 2. Effects of CPF and TETRA on the ratio of live, apoptotic and dead cells of K, U and J cybrids. (a,d,g,j) higher relative ratio of apoptotic and dead K cybrids via CPF and TETRA; (b,e,h,k) No significant change in ratio of apoptotic and dead cells via either treatment in U cybrids; (c,f,i,l) elevated ratio of apoptotic and dead J cybrids via CPF and TETRA.

3.5.1. K Cybrids

Inflammation genes: Performing qRT-PCR, in all experiments, the value of 1 is assigned to the vehicle-control samples. In terms of the pro-inflammatory gene pathway in K cybrids, the relative gene expression of *IL-33* ($p < 0.0001$) (Figure 3b) increased significantly with CPF treatment. There was higher expression of *IL-6* gene ($p < 0.0001$) (Figure 3a) with TETRA treatment compared to vehicle-control samples. However, TETRA treatment showed no effect on the *IL-33* (Figure 3b) and *TGF- β 1* gene expression levels (Figure 3c) compared to the vehicle-control group. Additionally, there was no alteration of *TGF- β 1* gene after CPF treatment (Figure 3c).

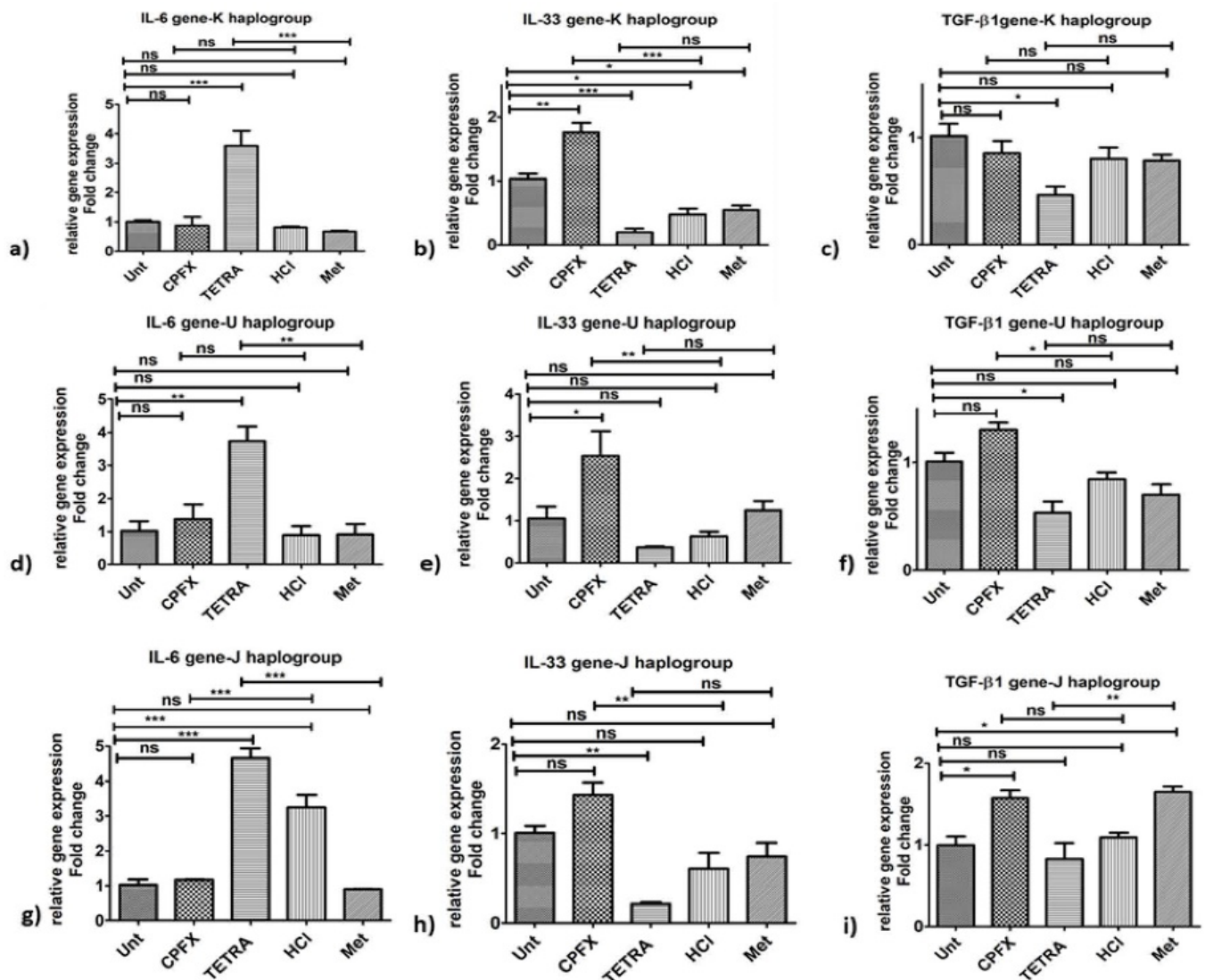


Figure 3. Changes in pro-inflammatory gene expression by CPF and TETRA in K, U and J cybrids. In K Cybrids, (a) overexpression of *IL-6* via TETRA, (b) higher *IL-33* expression via CPF; (c) and higher *TGF-β1* expression via CPF (c). In U cybrids, (d) higher *IL-6* expression via TETRA, (e) higher *IL-33* expression via CPF and (f) upregulation of *TGF-β1* via CPF. In J Cybrids, (g) lower expression of *IL-6* via CPF, (h) upregulation of *IL-33* via CPF; (i) and downregulation of *TGF-β1* via TETRA. (* $p < 0.05$, ** $p < 0.01$, *** $p < 0.0001$).

Pro-apoptosis genes: In K cybrids, CPF stimulated overexpression of *CASP-3* ($p < 0.0001$) (Figure 4a), *CASP-7* ($p < 0.0001$) (Figure 4b) and *CASP-9* ($p < 0.0001$) (Figure 4c), in comparison with vehicle-control samples. Similarly, after TETRA treatment, expression levels of *CASP-3* (Figure 4a) and *CASP-7* (Figure 4b) of K cybrids were upregulated ($p < 0.01$).

Antioxidant genes: The CPF-treated K cybrids showed no significant impacts on the expression levels of *SOD1* (Figure 5a), *SOD2* (Figure 5b), *SOD3* (Figure 5c) and *GPX3* (Figure 5d) genes. With TETRA treatment, there were lower expression levels of *SOD3* ($p < 0.01$) (Figure 5c) and *GPX3* ($p < 0.05$) (Figure 5d) genes in K cybrids versus vehicle-control-exposed samples.

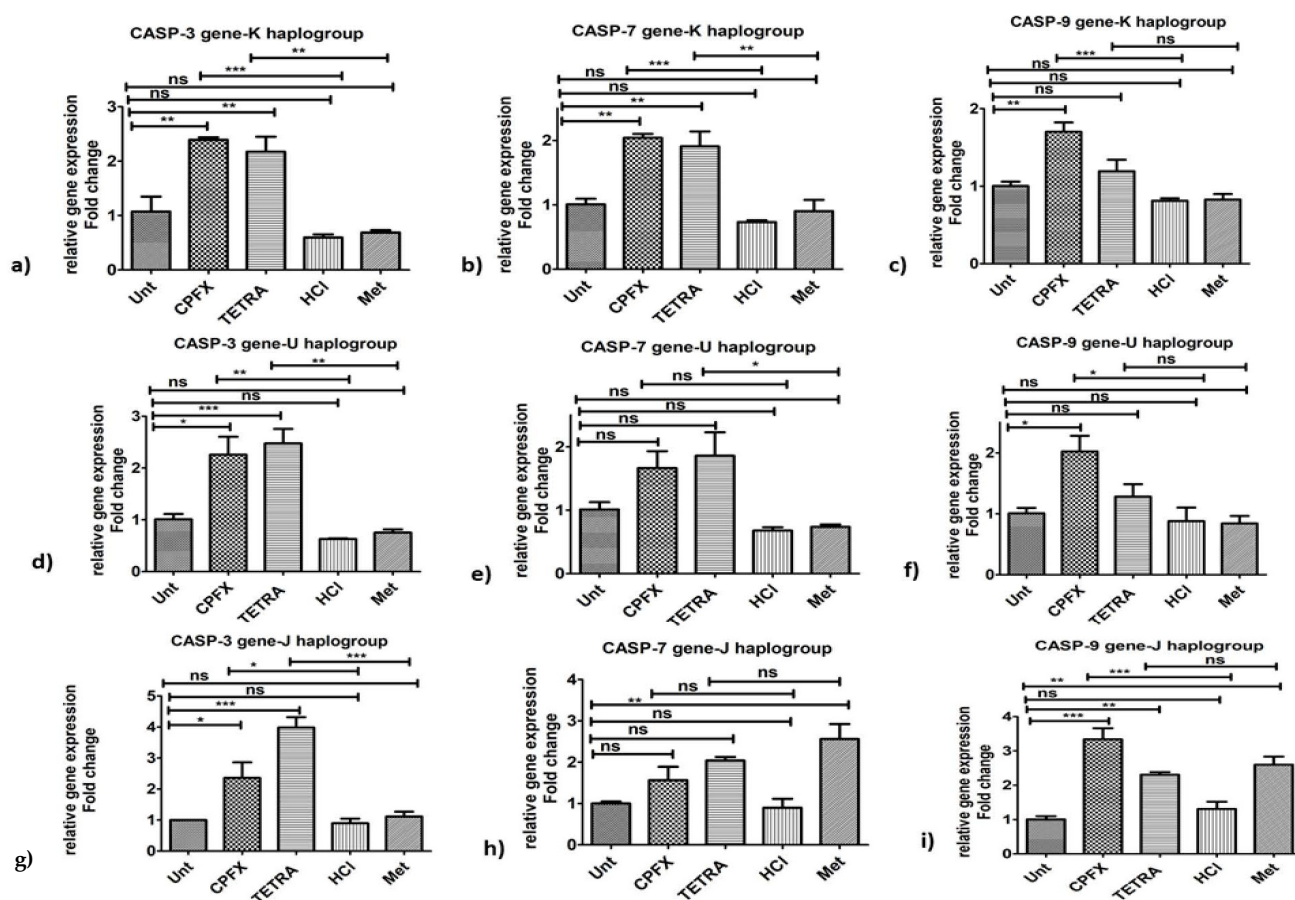


Figure 4. Alterations of pro-apoptotic genes induced by CPF and TETRA in K, U and J cybrids. Overexpression of *CASP-3* (a,d,g) via CPF and TETRA in all three cybrids and upregulation of *CASP-7* via CPF and TETRA in K haplogroup (b) and overexpression of *CASP-7* by TETRA in U cybrids (e,h) and higher *CASP-9* (c,f,i) expression by CPF in all three cybrids. (* $p < 0.05$, ** $p < 0.01$, *** $p < 0.0001$).

3.5.2. U Cybrids

Inflammation genes: The CPF-treated U cybrids showed upregulation of *IL-33* ($p < 0.01$) (Figure 3e) and *TGF- β 1* ($p < 0.05$) (Figure 3f), compared to vehicle-control cells. Although TETRA induced a higher expression level of *IL-6* ($p < 0.01$) (Figure 3d), the expression level of *IL-33* (Figure 3e) and *TGF- β 1* (Figure 3f) genes was not affected after TETRA treatment in U cybrids.

Pro-apoptosis genes: In comparison to vehicle-control cells, treated U cybrids with CPF showed significantly higher expression of *CASP-3* ($p < 0.01$) (Figure 4d) and *CASP-9* ($p < 0.05$) genes. However, there was no alteration of expression level of *CASP-7* (Figure 4e) in CPF-treated U cybrids. Furthermore, TETRA-treated U cybrids showed upregulation of *CASP-3* ($p < 0.01$) (Figure 4d) and *CASP-7* ($p < 0.05$) (Figure 4e) genes. The expression of *CASP-9* (Figure 4f) showed no significant alteration after TETRA treatment.

Antioxidant genes: The U cybrids showed higher expression levels of *SOD2* gene ($p < 0.01$) (Figure 5f) via TETRA. However, TETRA caused downregulation of *SOD3* gene in exposed U cybrids ($p < 0.05$) (Figure 5g). CPF exposure did not affect expression levels of *SOD2* (Figure 5f), *SOD3* (Figure 5g) and *GPX3* (Figure 5h) genes. Additionally, neither treatment altered the expression level of *SOD1* gene (Figure 5e).

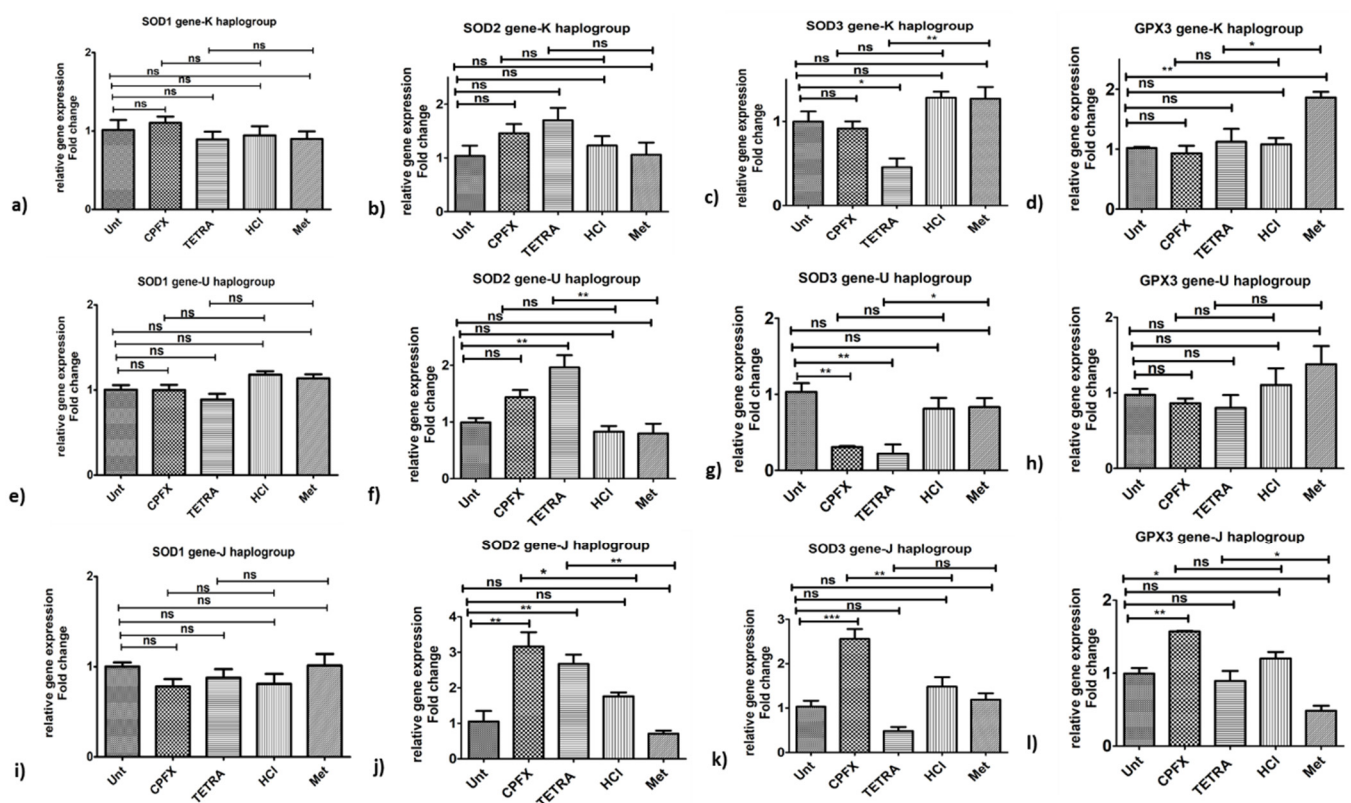


Figure 5. Impacts of CPF and TETRA on genomic expression of antioxidant enzymes in K, U and J cybrids. In K cybrids, (a,b) no significant change in *SOD1* and *SOD2* by either treatment, (c,d) downregulation of *SOD3* and *GPX3* by TETRA. In U cybrids, (e,h) no significant change in *SOD1* and *GPX3* by either treatment, (f) higher expression of *SOD2* and (g) lower expression of *SOD3* via TETRA. In J cybrids, (i) no significant change in *SOD1* by either treatment, (j) upregulation of *SOD2* via CPF and TETRA, (k) higher expression of *SOD3* by CPF, and (l) overexpression of *GPX3* by CPF. (* $p < 0.05$, ** $p < 0.01$, *** $p < 0.0001$).

3.5.3. J Cybrids

Inflammation genes: The CPF-treated J cybrids showed upregulation of *IL-33* ($p < 0.01$) (Figure 3h) but lower expression levels of *IL-6* ($p < 0.0001$) (Figure 3g) along with no effects on *TGF- β 1* ($p = 0.013$) (Figure 3i) genes. The TETRA-treated J cybrids showed an increased expression level of *IL-6* gene ($p < 0.0001$) (Figure 3g) along with downregulated expression of *TGF- β 1* ($p < 0.01$) (Figure 3i) and no alteration of *IL-33* (Figure 3h) genes.

Pro-apoptosis genes: CPF and TETRA treatment of J cybrids, increased expression level of *CASP-3* ($p < 0.05$) (Figure 4g) and *CASP-9* ($p < 0.0001$) (Figure 4i) genes, compared to vehicle-control group. Neither antibiotic altered the expression level of *CASP-7* gene in treated J cybrids (Figure 4h).

Antioxidant genes: The CPF-treated J cybrids showed substantial overexpression of *SOD2* ($p < 0.05$) (Figure 5j) and *SOD3* ($p < 0.01$) (Figure 5k) along with no alteration of *SOD1* (Figure 5i) and *GPX3* (Figure 5l), respectively, compared to vehicle-control samples. The TETRA treatment induced a higher expression level of *SOD2* ($p < 0.01$) (Figure 5j) and *GPX3* ($p < 0.05$) (Figure 5l) genes but no alteration of expression level of *SOD1* (Figure 5i) and *SOD3* genes (Figure 5k).

These results demonstrate that CPF and TETRA treatments affect the relative expression levels of various genes associated with inflammatory, apoptotic and antioxidant enzymes. Figure 6 summarizes the expression levels of genes associated with apoptotic, inflammatory and antioxidant enzymes after CPF and TETRA treatments.

K haplogroup		U haplogroup		J haplogroup	
CPF	TETRA	CPF	TETRA	CPF	TETRA
IL-6 ↔	↑↑↑	IL-6 ↔	↑↑	IL-6 ↓↓↓	↑↑↑
IL-33 ↑↑↑	↔	IL-33 ↑↑	↔	IL-33 ↑↑	↔
TGF-β1 ↔	↔	TGF-β1 ↑	↔	TGF-β1 ↔	↓↓
K haplogroup		U haplogroup		J haplogroup	
CPF	TETRA	CPF	TETRA	CPF	TETRA
CASP-3 ↑↑↑	↑↑	CASP-3 ↑↑	↑↑	CASP-3 ↑	↑↑↑
CASP-7 ↑↑↑	↑↑	CASP-7 ↔	↑	CASP-7 ↔	↔
CASP-9 ↑↑↑	↔	CASP-9 ↑	↔	CASP-9 ↑↑↑	↔
K haplogroup		U haplogroup		J haplogroup	
CPF	TETRA	CPF	TETRA	CPF	TETRA
SOD1 ↔	↔	SOD1 ↔	↔	SOD1 ↔	↔
SOD2 ↔	↔	SOD2 ↔	↑↑	SOD2 ↑	↑↑
SOD3 ↔	↓↓	SOD3 ↔	↓	SOD3 ↑↑	↔
GPX3 ↔	↓	GPX3 ↔	↔	GPX3 ↔	↑

Figure 6. The Summary of Changes in Gene Expression Influenced by CPF and TETRA Treatment Compared to Vehicle-Control Cells.

4. Discussion

Fluoroquinolones and tetracyclines have a wide range of antibacterial activities but previous studies have demonstrated possible ocular toxicities as a result of fluoroquinolone administration. In Canada, Etminan et al. conducted a case–control study on 989,591 patients with ophthalmic disease, who were followed between 2000 and 2007. They reported a higher risk of retinal detachment in patients who used oral fluoroquinolones (3.3% of cases) compared to the control group (0.6%) [38]. Another group concluded that the hazard of uveitis-associated systemic illnesses was higher in individuals treated with fluoroquinolones in the outpatient setting [39]. These findings suggest that the mitochondrial sensitivities to these antibiotics may play a role in the side effects seen in some patients. The present study investigates the effects of CPF and TETRA on cybrid cell lines that possess different mtDNA haplogroup patterns.

5. Effects of CPF on AMD Cybrids

Mitochondrial membrane potential and ROS levels after CPF treatment: Our findings indicate that different cybrid haplogroups respond differently to treatment with CPF; (i) There is a reduction in ROS levels in J haplogroup after treatment with CPF 120 µg/mL; (ii) all haplogroup cybrids showed decreased $\Delta\psi_M$ levels and lower cell metabolism with CPF 120 µg/mL treatment; additionally, (iii) all three haplogroups treated with CPF 120 µg/mL showed significantly elevated ratios of apoptotic and dead cells.

Other studies have also reported mitochondrial dysfunction and higher ROS levels after antibiotic exposure. Kalghatgi et al. assessed the effects of three bactericidal antibiotics (kanamycin, ciprofloxacin and ampicillin) and one bacteriostatic (tetracycline) on harvested mouse mammary tissues [26]. The bactericidal agents negatively affected mitochondria electron transportation chain (ETC), which led to significantly increased ROS levels and eventually cellular lipid, protein and DNA damage [26]. In another study, application of higher concentrations of fluoroquinolones and tetracycline impaired mitochondrial function in cultured primary human osteoblasts [40]. Similar harmful effects on mitochondria were

also shown in animal studies. For example, intraperitoneal injection of fluoroquinolones (alatrofloxacin) caused oxidative stress and mitochondrial injury in a Sod2+/- (heterozygous deficiency in mitochondrial superoxide dismutase, Sod2) mouse model. Compared to wild-type mice, there was a significant reduction in mitochondrial genes and critical enzyme activities in mutant models after injection of 33 mg/kg/day of alatrofloxacin over 28 days. Moreover, the activation of mitochondrial Ca²⁺ dependent mechanisms, such as nitric oxide (NOS) production, was more prominent in alatrofloxacin-treated mutant mice [41]. Multiple studies reported substantial structural and functional alterations of mitochondria in AMD subjects, including disorganized membranes, cristae and matrix along with reduction in mitochondria numbers [32,42,43]. Therefore, this harmful role of bactericidal agents could be more prominent in individuals suffering from an impaired antioxidant defense system along with patients with specific age-related disease with damaged mitochondria such as AMD and Parkinson's disease. By identifying eukaryotic mitochondrial dysfunction and over-production of ROS linked to fluoroquinolones, therapeutic approaches are progressing regarding alleviating the harmful side consequences of antibiotics administration [44].

Gene expression studies after CPFEX treatment: Exposure with CPFEX 120 µg/mL induced (i) overexpression of *IL-33* in all treated haplogroups; and (ii) upregulation of *CASP-3* and *CASP-9* genes in all exposed haplogroups. Prior literature has shown considerable retinal damage due to increased phototoxicity after fluoroquinolone intake. The phototoxicity of five different fluoroquinolones (ciprofloxacin, enoxacin, DR-3355 (the s-isomer of ofloxacin), lomefloxacin and ofloxacin) was demonstrated in culture mouse 3T3 fibroblast cells exposed to ultraviolet-A (UVA) light [45].

Cellular apoptosis has been described as the mechanism associated with the cytotoxic properties of fluoroquinolones. Kohanski et al. compared the ROS levels in *Escherichia coli* produced via three various categories of bactericidal agents including 250 ng/mL norfloxacin, 5 µg/mL kanamycin and 5 µg/mL ampicillin compared to bacteriostatic ones including tetracycline, erythromycin, spectinomycin and chloramphenicol treatments. It was indicated that the bactericidal groups induced higher deleterious production of hydroxyl radicals contributing oxidative damage and cellular death [46]. To our knowledge, this is the first study to measure the effects of CPFEX treatment on expression patterns of genes associated with basic pathways.

Effects of TETRA on AMD Cybrids

Mitochondrial membrane potential and ROS levels after TETRA treatment: Our results demonstrated: (i) significantly diminished ROS levels in U and J haplogroup cybrids via TETRA 120 µg/mL; (ii) declining levels of $\Delta\psi_M$ with all TETRA treatment concentrations in all three haplogroups; (iii) diminished cellular metabolism of treated K and J haplogroups cybrids after TETRA 30 µg/mL; and (iv) significant increase in the ratio of dead cells of K and J haplogroups treated with TETRA 120 µg/mL. Similar detrimental effects have been reported by Ding et al. who showed the toxicity of a series of concentrations (0, 45, 60 and 90 mg/L) of two types tetracyclines (doxycycline and chlortetracycline) and four fluoroquinolones (enrofloxacin, norfloxacin, ciprofloxacin and ofloxacin) on wild-type zebrafish. It was suggested that over 7-, 14- and 21-day exposure periods, there was a significant decrease in mitochondria crista along with severe mitochondria swelling in the treated subjects [47]. Another study in agreement with our results investigated the role of doxycycline on the proliferation and metabolism of in vitro breast epithelial lines (MCF12A) [48]. Moreover, the similar risk and mitochondrial-damaging mechanisms are identified as a consequence of topical administration of tetracyclines [49].

Expression studies after TETRA treatment: Our findings showed cybrids treated with TETRA 120 µg/mL had (i) up-regulation of *IL-6* and *CASP-3* levels in all haplogroups; but (ii) down-regulation of *IL-33* and *SOD3* genes in K and U haplogroup cybrids. Ahler et al. studied the impacts of doxycycline on alteration of proliferation and metabolism of multiple human cell lines in vitro, such as cervical cancer cells (Hela), lung cancer cells

(H157) and prostate cancer cells (LNCaP). There was a widespread alteration of expression of genes associated with the oxidative metabolic pathway along with dominance of the glycolytic metabolism pathway [50]. They examined expression levels of genes associated with gluconeogenesis (fructose-1,6-bisphosphatase (*FBP*) and glucose-6-phosphatase (*G6PC*)) along with regulatory enzymes of the glycolysis pathway (pyruvate kinase (*PK*), hexokinase (*HK*) and phosphofructokinase (*PFK*)). They reported downregulation after TETRA treatment of the *G6PC* and *FBP* genes, along with upregulatory effects on *PK* gene levels [49]. In our study, the principal enzymes related to the antioxidant pathway were affected by treatments. TETRA 120 µg/mL induced downregulation of *SOD2* expression in U and J haplogroups along with lower expression of *GPX3* in exposed K haplogroups. Noteworthy, Jones et al. reported the importance of the disruptive role of tetracyclines in individuals with mitochondrial defects. The fibroblast cells derived from four categories of patients with defective mitochondrial diseases were exposed to doxycycline (10 µg/mL) or tetracycline (77 µg/mL). There was significant disruption of mitochondrial translation resulting from exposure to these antibiotics [50].

6. Conclusions

In light of these results, the clinically relevant dosages of bactericidal and bacteriostatic agents showed detrimental effects on treated in vitro AMD cybrid cell lines. The negative association of antibiotics and mitochondria might be important in populations suffering from age-related disorders that are associated with damaged mitochondria, such as AMD, Parkinson's and Alzheimer's diseases. In the future, additional in vivo and clinical trials may need to be conducted to improve our understanding and knowledge regarding the negative contributory roles of these antibiotics on mitochondrial dysfunction.

7. Strength and Limitations of the Study

The findings of this study might be significant in clinical settings, particularly regarding the approach to treat the patients suffering from specific age-related disease such as AMD, Parkinson's disease and Alzheimer's disease. The only limitation of the study is the smaller cohort of individuals with AMD for three different cybrid cell lines.

Author Contributions: N.S. and M.C.K. were responsible for the conception and design of the work; N.S. performed all the experiments; M.C.K., M.C. and S.R.A. contributed the acquisition, analysis, and interpretation of data for the work; B.D.K., S.Y.L. and M.C. contributed to creation of the cybrids; L.S. and M.K.S. helped in the manuscript preparation. Z.M., A.B.N., S.Y.L. and M.C.K. reviewed the manuscript. All authors have read and agreed to the published version of the manuscript.

Funding: This research was funded by Discovery Eye Foundation, Polly and Michael Smith, Edith and Roy Carver, Iris and B. Gerald Cantor Foundation, Max Factor Family Foundation, and NEI R01 EY027363 (MCK). Supported in part by an Unrestricted Departmental Grant from Research to Prevent Blindness. We acknowledge the support of the Institute for Clinical and Translational Science (ICTS) at University of California Irvine (ULI TR001414/TR/NCATS). NS was a Beckman Foundation Fellow in Retinal Degeneration Research.

Institutional Review Board Statement: Not applicable.

Informed Consent Statement: In terms of various phases of this study including designing, performing and revealing of the results, patients or the public were not involved.

Data Availability Statement: All data relevant to the study are included in the article.

Conflicts of Interest: B.D.K. is consultant to Alcon, Alimera, Allegro, Allergan, Genentech, Glaukos, GSK, Neurotech, Novagali, Novartis, Ophthotech, Pfizer, Regeneron, Santen, SecondSight, Teva, ThromboGenics. The rest of the authors declare that they have no competing interests. The funders had no role in the design of the study; in the collection, analyses, or interpretation of data; in the writing of the manuscript, or in the decision to publish the results.

References

1. Katz, L.; Baltz, R.H. Natural product discovery: Past, present, and future. *J. Ind. Microbiol. Biotechnol.* **2016**, *43*, 155–176. [[CrossRef](#)] [[PubMed](#)]
2. Hutchings, M.I.; Truman, A.W.; Wilkinson, B. Antibiotics: Past, present and future. *Curr. Opin. Microbiol.* **2019**, *51*, 72–80. [[CrossRef](#)] [[PubMed](#)]
3. Prescott, J.F. The resistance tsunami, antimicrobial stewardship, and the golden age of microbiology. *Vet. Microbiol.* **2014**, *171*, 273–278. [[CrossRef](#)] [[PubMed](#)]
4. Smith, A.; Pennefather, P.M.; Kaye, S.B.; Hart, C.A. Fluoroquinolones. *Drugs* **2001**, *61*, 747–761. [[CrossRef](#)] [[PubMed](#)]
5. Pan, X.-S.; Fisher, L.M. Targeting of DNA gyrase in *Streptococcus pneumoniae* by sparfloxacin: Selective targeting of gyrase or topoisomerase IV by quinolones. *Antimicrob. Agents Chemother.* **1997**, *41*, 471–474. [[CrossRef](#)] [[PubMed](#)]
6. Lewis, T.; Cook, J. Fluoroquinolones and tendinopathy: A guide for athletes and sports clinicians and a systematic review of the literature. *J. Athl. Train.* **2014**, *49*, 422–427. [[CrossRef](#)] [[PubMed](#)]
7. Falagas, M.E.; Rafailidis, P.I.; Rosmarakis, E.S. Arrhythmias associated with fluoroquinolone therapy. *Int. J. Antimicrob. Agents* **2007**, *29*, 374–379. [[CrossRef](#)]
8. Samarakoon, N.; Harrisberg, B.; Ell, J. Ciprofloxacin-induced toxic optic neuropathy. *Clin. Exp. Ophthalmol.* **2007**, *35*, 102–104. [[CrossRef](#)]
9. Fife, D.; Zhu, V.; Voss, E.; Levy-Clarke, G.; Ryan, P. Exposure to oral fluoroquinolones and the risk of retinal detachment: Retrospective analyses of two large healthcare databases. *Drug Saf.* **2014**, *37*, 171–182. [[CrossRef](#)]
10. Roberts, M.C. Tetracyclines: Mode of action and their bacterial mechanisms of resistance. *Bact. Resist. Antibiot. Mol. Man* **2019**, 101–124.
11. Sapadin, A.N.; Fleischmajer, R. Tetracyclines: Nonantibiotic properties and their clinical implications. *J. Am. Acad. Dermatol.* **2006**, *54*, 258–265. [[CrossRef](#)] [[PubMed](#)]
12. Dougherty, J.M.; McCulley, J.P.; Silvany, R.E.; Meyer, D.R. The role of tetracycline in chronic blepharitis. Inhibition of lipase production in staphylococci. *Investig. Ophthalmol. Vis. Sci.* **1991**, *32*, 2970–2975.
13. Sandler, C.; Ekokoski, E.; Lindstedt, K.A.; Vainio, P.; Finel, M.; Sorsa, T.; Kovanen, P.T.; Golub, L.; Eklund, K.K. Chemically modified tetracycline (CMT)-3 inhibits histamine release and cytokine production in mast cells: Possible involvement of protein kinase C. *Inflamm. Res.* **2005**, *54*, 304–312. [[CrossRef](#)]
14. Chopra, I.; Roberts, M. Tetracycline antibiotics: Mode of action, applications, molecular biology, and epidemiology of bacterial resistance. *Microbiol. Mol. Biol. Rev.* **2001**, *65*, 232–260. [[CrossRef](#)]
15. Zakeri, B.; Wright, G.D. Chemical biology of tetracycline antibiotics. *Biochem. Cell Biol.* **2008**, *86*, 124–136. [[CrossRef](#)] [[PubMed](#)]
16. Sodhi, M.; Etminan, M. Therapeutic Potential for Tetracyclines in the Treatment of COVID-19. *Pharmacotherapy* **2020**, *40*, 487. [[CrossRef](#)]
17. Sandler, C.; Nurmi, K.; Lindstedt, K.A.; Sorsa, T.; Golub, L.M.; Kovanen, P.T.; Eklund, K.K. Chemically modified tetracyclines induce apoptosis in cultured mast cells. *Int. Immunopharmacol.* **2005**, *5*, 1611–1621. [[CrossRef](#)]
18. Sánchez, A.R.; Rogers, R.S., III; Sheridan, P.J. Tetracycline and other tetracycline-derivative staining of the teeth and oral cavity. *Int. J. Dermatol.* **2004**, *43*, 709–715. [[CrossRef](#)]
19. Hamblin, M.R.; Abrahamse, H. Tetracyclines: Light-activated antibiotics? *Future Med. Chem.* **2019**, *11*, 2427–2445. [[CrossRef](#)]
20. Wallace, I.; Krupin, T.; Stone, R.; Moolchandani, J. The ocular hypotensive effects of demeclocycline, tetracycline and other tetracycline derivatives. *Investig. Ophthalmol. Vis. Sci.* **1989**, *30*, 1594–1598.
21. Tielens, A.G.; Rotte, C.; van Hellemond, J.J.; Martin, W. Mitochondria as we don't know them. *Trends Biochem. Sci.* **2002**, *27*, 564–572. [[CrossRef](#)]
22. McBride, H.M.; Neuspiel, M.; Wasiak, S. Mitochondria: More than just a powerhouse. *Curr. Biol.* **2006**, *16*, R551–R560. [[CrossRef](#)] [[PubMed](#)]
23. Gray, M.W.; Burger, G.; Lang, B.F. Mitochondrial evolution. *Science* **1999**, *283*, 1476–1481. [[CrossRef](#)] [[PubMed](#)]
24. Andersson, G.; Karlberg, O.; Canbäck, B.; Kurland, C.G. On the origin of mitochondria: A genomics perspective. *Philos. Trans. R. Soc. London. Ser. B: Biol. Sci.* **2003**, *358*, 165–179. [[CrossRef](#)] [[PubMed](#)]
25. Boguszewska, K.; Szewczuk, M.; Kaźmierczak-Barańska, J.; Karwowski, B.T. The similarities between human mitochondria and bacteria in the context of structure, genome, and base excision repair system. *Molecules* **2020**, *25*, 2857. [[CrossRef](#)] [[PubMed](#)]
26. Kalghatgi, S.; Spina, C.S.; Costello, J.C.; Liesa, M.; Morones-Ramirez, J.R.; Slomovic, S.; Molina, A.; Shirihai, O.S.; Collins, J.J. Bactericidal antibiotics induce mitochondrial dysfunction and oxidative damage in mammalian cells. *Sci. Transl. Med.* **2013**, *5*, 192ra185. [[CrossRef](#)]
27. Kenney, M.C.; Atilano, S.R.; Boyer, D.; Chwa, M.; Chak, G.; Chinichian, S.; Coskun, P.; Wallace, D.C.; Nesburn, A.B.; Udar, N.S. Characterization of retinal and blood mitochondrial DNA from age-related macular degeneration patients. *Investig. Ophthalmol. Vis. Sci.* **2010**, *51*, 4289–4297. [[CrossRef](#)]
28. Salimiaghdam, N.; Singh, L.; Schneider, K.; Nalbandian, A.; Chwa, M.; Atilano, S.R.; Bao, A.; Kenney, M.C. Potential adverse effects of ciprofloxacin and tetracycline on ARPE-19 cell lines. *BMJ Open Ophthalmol.* **2020**, *5*, e000458. [[CrossRef](#)]
29. Salimiaghdam, N.; Singh, L.; Schneider, K.; Chwa, M.; Atilano, S.R.; Nalbandian, A.; Limb, G.A.; Kenney, M.C. Effects of fluoroquinolones and tetracyclines on mitochondria of human retinal MIO-M1 cells. *Exp. Eye Res.* **2022**, *214*, 108857. [[CrossRef](#)]

30. Salimiaghdam, N.; Riazi-Esfahani, M.; Fukuhara, P.S.; Schneider, K.; Kenney, M.C. Age-related macular degeneration (AMD): A review on its epidemiology and risk factors. *Open Ophthalmol. J.* **2019**, *13*, 90–99. [[CrossRef](#)]
31. Musiał-Kopiejka, M.; Polanowska, K.; Dobrowolski, D.; Krysik, K.; Wylęgała, E.; Grabarek, B.O.; Lyssek-Boroń, A. The Effectiveness of Brolicizumab and Aflibercept in Patients with Neovascular Age-Related Macular Degeneration. *Int. J. Env. Res. Public Health* **2022**, *19*, 2303. [[CrossRef](#)] [[PubMed](#)]
32. Kenney, M.C.; Chwa, M.; Atilano, S.R.; Pavlis, J.M.; Falatoonzadeh, P.; Ramirez, C.; Malik, D.; Hsu, T.; Woo, G.; Soe, K. Mitochondrial DNA variants mediate energy production and expression levels for CFH, C3 and EFEMP1 genes: Implications for age-related macular degeneration. *PLoS ONE* **2013**, *8*, e54339. [[CrossRef](#)] [[PubMed](#)]
33. Mueller, E.E.; Schaier, E.; Brunner, S.M.; Eder, W.; Mayr, J.A.; Egger, S.F.; Nischler, C.; Oberkofler, H.; Reitsamer, H.A.; Patsch, W. Mitochondrial haplogroups and control region polymorphisms in age-related macular degeneration: A case-control study. *PLoS ONE* **2012**, *7*, e30874. [[CrossRef](#)] [[PubMed](#)]
34. Kenney, M.C.; Chwa, M.; Atilano, S.R.; Falatoonzadeh, P.; Ramirez, C.; Malik, D.; Tarek, M.; Cáceres-del-Carpio, J.; Nesburn, A.B.; Boyer, D.S. Inherited mitochondrial DNA variants can affect complement, inflammation and apoptosis pathways: Insights into mitochondrial–nuclear interactions. *Hum. Mol. Genet.* **2014**, *23*, 3537–3551. [[CrossRef](#)]
35. Dunn, K.; Aotaki-Keen, A.; Putkey, F.; Hjelmeland, L.M. ARPE-19, a human retinal pigment epithelial cell line with differentiated properties. *Exp. Eye Res.* **1996**, *62*, 155–170. [[CrossRef](#)] [[PubMed](#)]
36. Miceli, M.V.; Jazwinski, S.M. Nuclear gene expression changes due to mitochondrial dysfunction in ARPE-19 cells: Implications for age-related macular degeneration. *Investig. Ophthalmol. Vis. Sci.* **2005**, *46*, 1765–1773. [[CrossRef](#)]
37. Asiabi, P.; Ambroise, J.; Giachini, C.; Coccia, M.; Bearzatto, B.; Chiti, M.C.; Dolmans, M.-M.; Amorim, C. Assessing and validating housekeeping genes in normal, cancerous, and polycystic human ovaries. *J. Assist. Reprod. Genet.* **2020**, *37*, 2545–2553. [[CrossRef](#)]
38. Etminan, M.; Forooghian, F.; Brophy, J.M.; Bird, S.T.; Maberley, D. Oral fluoroquinolones and the risk of retinal detachment. *JAMA* **2012**, *307*, 1414–1419.
39. Nacht, J. Oral Fluoroquinolones and the Risk Of Uveitis. *J. Emerg. Med.* **2016**, *5*, 805–806. [[CrossRef](#)]
40. Duetzelhenke, N.; Krut, O.; Eysel, P. Influence on mitochondria and cytotoxicity of different antibiotics administered in high concentrations on primary human osteoblasts and cell lines. *Antimicrob. Agents Chemother.* **2007**, *51*, 54–63. [[CrossRef](#)]
41. Hsiao, C.-J.J.; Younis, H.; Boelsterli, U.A. Trovafloxacin, a fluoroquinolone antibiotic with hepatotoxic potential, causes mitochondrial peroxynitrite stress in a mouse model of underlying mitochondrial dysfunction. *Chem. Biol. Interact.* **2010**, *188*, 204–213. [[CrossRef](#)] [[PubMed](#)]
42. Karunadharma, P.P.; Nordgaard, C.L.; Olsen, T.W.; Ferrington, D.A. Mitochondrial DNA damage as a potential mechanism for age-related macular degeneration. *Investig. Ophthalmol. Vis. Sci.* **2010**, *51*, 5470–5479. [[CrossRef](#)] [[PubMed](#)]
43. Feher, J.; Kovacs, I.; Artico, M.; Cavallotti, C.; Papale, A.; Gabrieli, C.B. Mitochondrial alterations of retinal pigment epithelium in age-related macular degeneration. *Neurobiol. Aging* **2006**, *27*, 983–993. [[CrossRef](#)] [[PubMed](#)]
44. Hangas, A.; Aasumets, K.; Kekäläinen, N.J.; Paloheinä, M.; Pohjoismäki, J.L.; Gerhold, J.M.; Goffart, S. Ciprofloxacin impairs mitochondrial DNA replication initiation through inhibition of Topoisomerase 2. *Nucleic Acids Res.* **2018**, *46*, 9625–9636. [[CrossRef](#)]
45. Wagai, N.; Tawara, K. Possible direct role of reactive oxygens in the cause of cutaneous phototoxicity induced by five quinolones in mice. *Arch. Toxicol.* **1992**, *66*, 392–397. [[CrossRef](#)]
46. Kohanski, M.A.; Dwyer, D.J.; Hayete, B.; Lawrence, C.A.; Collins, J.J. A common mechanism of cellular death induced by bactericidal antibiotics. *Cell* **2007**, *130*, 797–810. [[CrossRef](#)]
47. Ding, L.; Zang, L.; Zhang, Y.; Zhang, Y.; Wang, X.; Ai, W.; Ding, N.; Wang, H. Joint toxicity of fluoroquinolone and tetracycline antibiotics to zebrafish (*Danio rerio*) based on biochemical biomarkers and histopathological observation. *J. Toxicol. Sci.* **2017**, *42*, 267–280. [[CrossRef](#)]
48. Ahler, E.; Sullivan, W.J.; Cass, A.; Braas, D.; York, A.G.; Bensinger, S.J.; Graeber, T.G.; Christofk, H.R. Doxycycline alters metabolism and proliferation of human cell lines. *PLoS ONE* **2013**, *8*, e64561.
49. Glickman, R.D. Phototoxicity to the retina: Mechanisms of damage. *Int. J. Toxicol.* **2002**, *21*, 473–490. [[CrossRef](#)]
50. Jones, C.N.; Miller, C.; Tenenbaum, A.; Spremulli, L.L.; Saada, A. Antibiotic effects on mitochondrial translation and in patients with mitochondrial translational defects. *Mitochondrion* **2009**, *9*, 429–437. [[CrossRef](#)]